International Journal of Biology and Life Sciences
ISSN: 2957-9511 | Vol. 16, No. 2, 2026

Pan-cancer Expression Analysis of *CXCL1/8/10* and Their Relationship with Prognosis and Tumor Microenvironment

Peng Xie, Zhuizhui Jiao, Tingting Yin *

Xinjiang Vocational University of Technology, Kashgar, Xinjiang, China
*** Corresponding author:** Tingting Yin (Email: 2638687109@qq.com)

Abstract: ***Objective*** To analyze the expression characteristics and prognostic value of *CXCL* family members (*CXCL1/8/10*) across pan-cancer using bioinformatics approaches. ***Methods*** Transcriptomic and clinical data of 33 tumor types were obtained from the TCGA database. Differential expression was evaluated by the Wilcoxon rank-sum test. Prognostic significance was assessed using Kaplan-Meier survival curves and univariate Cox regression. Spearman correlation analysis was applied to examine associations with immune subtypes, tumor stemness scores, tumor microenvironment (TME) components, tumor mutational burden (TMB), and microsatellite instability (MSI). ***Results*** *CXCL1/8/10* exhibited marked expression heterogeneity across cancer types, with *CXCL10* showing relatively high expression in the majority of tumors. The expression levels of all three genes were significantly associated with overall survival and showed varying degrees of correlation with immune infiltration subtypes, stromal/immune scores, and tumor stemness scores. After adjusting for tumor purity, the correlations between *CXCL10* and TMB/MSI remained significant in several cancer types. ***Conclusion*** *CXCL1/8/10* display significant expression heterogeneity in pan-cancer and are closely associated with the immune microenvironment and tumor stemness, representing potential prognostic biomarkers and therapeutic targets for specific cancer types.

Keywords: *CXCL1/8/10*; Pan-cancer; Tumor Microenvironment; Stemness Index; Bioinformatics.

1. Introduction

CXC chemokines constitute a family of small secreted proteins characterized by a single non-cysteine residue between the first two cysteines. This structure serves not only as the basis for classifying the *CXC* subfamily but is also closely related to their biological functions [1]. CXC chemokines mainly bind to G protein-coupled receptors and transmit signals into the cell, inducing the directional migration and activation of immune cells such as white blood cells [2-3]. In tumor biology, *CXC* chemokines have multiple regulatory effects, by recruiting immune cells such as neutrophils and T cells into the tumor microenvironment, regulating the infiltration level and functional state of immune cells, and thereby affecting tumor proliferation, invasion, angiogenesis, and treatment resistance [1-4]. These chemokines also participate in shaping the tumor immune microenvironment, regulating immune cell infiltration and activation in ways that affect tumor growth and metastasis, and contributing to immune escape mechanisms [3,4].

CXCL1, CXCL8, and *CXCL10* are prominent members of this family that belong to distinct CXC chemokine subgroups and differ in receptor selectivity and functional properties. Previous studies have reported that high expression of *CXCL1* and *CXCL8* correlates with tumor aggressiveness, metastasis, and unfavorable prognosis [4], while *CXCL10* regulates T cell recruitment through the CXCR3 receptor and plays a dual role in anti-tumor immunity. However, systematic comparative studies of these chemokines in multiple cancer types are still relatively insufficient, and the differences in expression patterns, prognostic directions and microenvironmental associations between different types of tumors have not yet been clarified. Therefore, in-depth exploration of the role of *CXCL1/8/10* in the tumor immune microenvironment is of great significance for revealing the molecular basis of tumor immune escape and developing new immunotherapy targets. In this study, transcriptomic and clinical data for 33 TCGA tumor types and their adjacent normal tissues were retrieved from the UCSC Xena database to systematically analyze the expression profiles of *CXCL1/8/10* in pan-cancer. Kaplan-Meier survival analysis and Cox regression were used to evaluate clinical associations, and multidimensional correlation analyses were performed to explore relationships between transcript levels and immune subtypes, stemness features, and the tumor microenvironment.

2. Materials and Methods

2.1. Characterization of *CXC* Chemokines

A phylogenetic tree of *CXC* chemokines was constructed using MEGA software with the neighbor-joining method and 1,000 bootstrap replicates to assess branch reliability [5], visualized with TBtools [6]. To represent the evolutionary relationships among *CXC* chemokine family members, five representative members (*CXCL1, CXCL2, CXCL8, CXCL9,* and *CXCL10*) were selected for phylogenetic analysis. These members belong to the ELR+ (*CXCL1, CXCL2, CXCL8*) and ELR- (*CXCL9, CXCL10*) subgroups, respectively, and collectively capture the major functional branches of the family. GFF3 files were downloaded from the NCBI database for gene structure analysis. Conserved motifs were identified using the MEME web server, and gene structures of the above members were parsed with TBtools. Tertiary structure prediction was performed using the SWISS-MODEL Interactive Workshop [7,8].

2.2. Differential Expression Analysis of *CXCL1/8/10* in Pan-cancer

RNA-seq (FPKM) gene expression profiles for 33 cancer types were downloaded from the UCSC Xena database, along with clinical, pathological, immune subtype, survival, and stemness score data [9]. The inclusion criterion was TCGA tumor samples with transcriptomic data and matched clinical information; datasets with fewer than five adjacent normal (control) samples and samples lacking complete follow-up information were excluded. *CXCL1, CXCL8,* and *CXCL10* expression profiles were extracted and integrated using Perl. Differential expression between tumor and adjacent normal tissues was assessed by the Wilcoxon rank-sum test, with P values adjusted for multiple comparisons using the Benjamini-Hochberg method. Adjusted P.adj < 0.05 and |log2FC| >= 1 were defined as the threshold for differential expression. Spearman correlation among the three genes was computed using the R package corrplot.

2.3. Survival Analysis based on *CXCL1/8/10* Expression

Survival data for each patient were extracted from the TCGA database to examine the relationship between *CXCL1/8/10* expression and clinical outcomes. Kaplan-Meier (KM) survival curves and log-rank tests (P < 0.05) were used for survival analysis, with patients stratified into high- and low-expression groups based on the median expression level of *CXCLs* in each tumor type. Survival curves were plotted using the R packages survminer and survival. Univariate Cox regression was performed to evaluate the association between *CXCL1/8/10* expression and overall survival across cancer types. Forest plots were generated using the R packages survival and forestplot to display hazard ratios (HR) and 95% confidence intervals.

2.4. Multidimensional Correlation Analysis of *CXCL1/8/10* in Pan-cancer

The associations between *CXCL1/8/10* expression and the tumor microenvironment, stemness scores, immune subtypes, TMB, and MSI were further analyzed: (1) TME scoring: Stromal and immune scores were calculated using the R packages estimate and limma to assess cellular infiltration in pan-cancer tissues; tumor purity was also computed and its correlation with *CXCL1/8/10* expression evaluated. (2) Stemness scores: Spearman correlation analysis, using the cor.test and limma packages, was applied to examine the relationships between *CXCL1/8/10* expression and RNA stemness score (RNAss) as well as DNA stemness score (DNAss) [10], with results visualized by corrplot. (3) Immune subtypes: Associations between *CXCL1/8/10* and six cancer immune subtypes were analyzed using the limma package, with group differences assessed by the Kruskal-Wallis test. (4) TMB/MSI associations: TMB and MSI scores were calculated from TCGA pan-cancer mutation data. Spearman partial correlation analysis, controlling for tumor purity, was used to evaluate the correlations between *CXCL1/8/10* expression (with a focus on *CXCL10*) and both metrics, with radar plots generated using the fmsb package. Correlation strength was defined as: |r| >= 0.7 strong, 0.4 <= |r| < 0.7 moderate, 0.2 <= |r| < 0.4 weak, and |r| < 0.2 negligible or absent.

2.5. Statistical Methods

All statistical analyses were performed in R (version 4.1.2). Between-group expression differences were compared using the Wilcoxon rank-sum test with Benjamini-Hochberg correction, defining differential expression as P.adj < 0.05 and |log2FC| >= 1. Survival analysis employed the Kaplan-Meier method and log-rank test; prognostic independence was assessed by univariate Cox proportional hazards regression, with effect sizes reported as HR and 95% CI. Multi-group comparisons used the Kruskal-Wallis test. Correlations were evaluated using Spearman coefficients, and partial correlation analysis controlling for tumor purity was applied in TMB/MSI analyses. Unless otherwise stated, P < 0.05 was considered statistically significant. R packages used included limma, survival, survminer, forestplot, estimate, corrplot, and fmsb.

3. Results

3.1. Gene Structure and Motif Composition of CXC Chemokines

To investigate the molecular characteristics and evolutionary relationships of the human *CXC* chemokine family, amino acid sequences of five representative members (*CXCL1, CXCL2, CXCL8, CXCL9,* and *CXCL10,* covering both ELR+ and ELR- subgroups) were used to construct a phylogenetic tree. The results showed that the above members could be divided into three subgroups (A, B, and C), with group A and group C each containing two members, and Group B containing only *CXCL8* (Figure 1a), suggesting that *CXCL8* may have a unique evolutionary path or functional differentiation. To further explore the molecular basis of functional differentiation, the conserved motifs of five proteins were predicted, and a total of 10 motifs (Motif 1-10) were identified. The results showed that *CXCL1* and *CXCL2* shared Motifs 1, 2, 3, and 6, indicating that their functions were highly similar. Additionally, the composition of motifs was related to the phylogenetic grouping: Group B (*CXCL8*) contained the fewest motifs (only 2), while Group C (*CXCL9*, *CXCL10*) had the most motifs and included unique Motifs 4, 5, 7, and 8 (Figure 1b), suggesting that the acquisition or loss of motifs might be one of the factors leading to functional differentiation. Exon-intron structure and predicted tertiary structures further confirmed appreciable differences among subgroups (Figure 1c, d). Based on these phylogenetic results, *CXCL1*, *CXCL8*, and *CXCL10*, which belong to different subgroups (A, B, and C) and exhibit representative differences in sequence features and motif composition, were selected as candidate genes for subsequent pan-cancer analysis.

3.2. Expression Levels of *CXCL1/8/10* in Pan-cancer

To explore the expression profiles of *CXCL1/8/10*, their expression levels were examined across 33 TCGA tumor types. *CXCL10* showed higher overall expression than *CXCL1* and CXCL8 in the majority of cancer types (Figure 2a). Co-expression analysis revealed a significant positive correlation between *CXCL1* and *CXCL8* (Spearman r = 0.79, P < 0.001), while *CXCL1* and *CXCL10* (r = 0.27, P < 0.001) and *CXCL8* and *CXCL10* (r = 0.25, P < 0.001) displayed only weak correlations (Figure 2b). These results suggest a potential cooperative relationship between *CXCL1* and

CXCL8 in transcriptional regulation, whereas *CXCL10* appears to be regulated more independently.

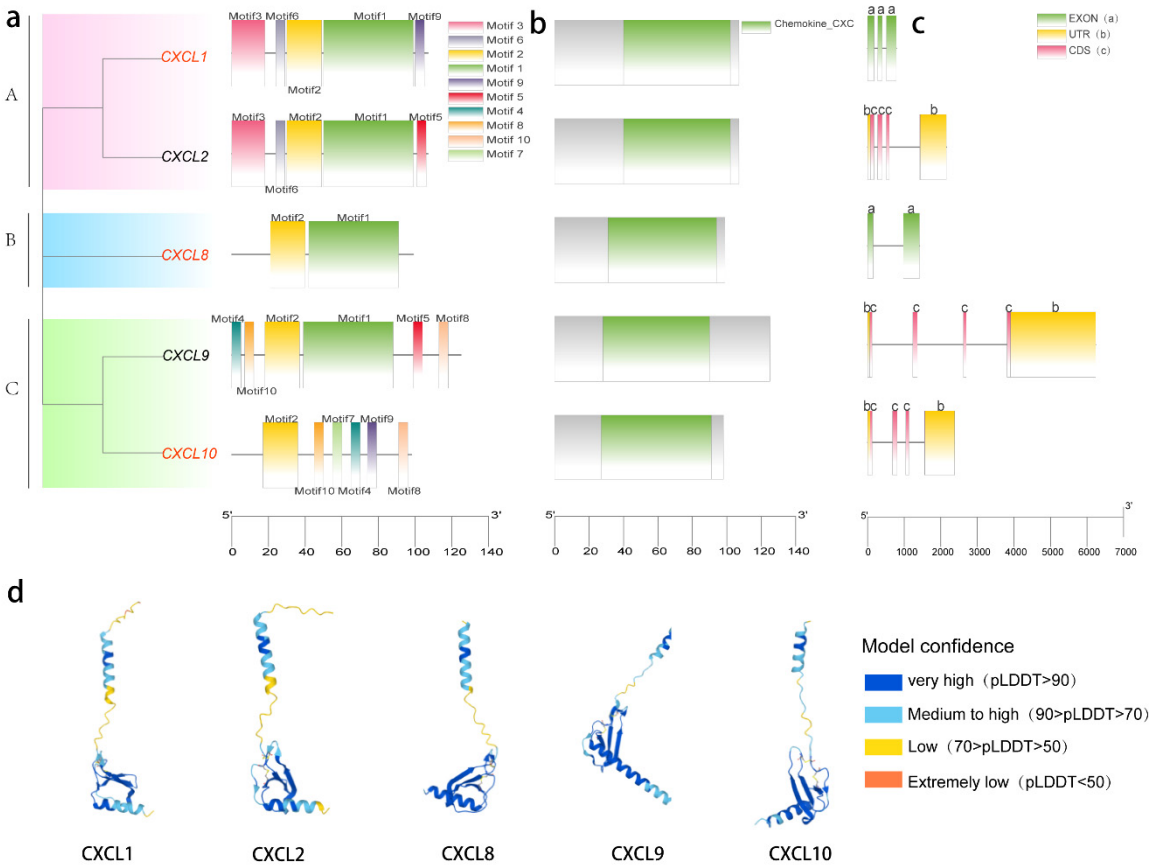

Figure 1. Phylogenetic relationships, conserved protein motifs, gene structures, and three-dimensional structural domains of CXC chemokines

(a) Phylogenetic tree based on full-length *CXC* chemokine protein sequences; A, B, and C represent the three groups. (b) Motif distribution of *CXC* chemokine proteins. (c) Exon-intron structures of *CXC* chemokines. (d) Three-dimensional structural domains of *CXC* chemokine proteins, with model quality indicated by plDDT confidence scores (plDDT > 90 high confidence, 70-90 moderately high, 50-70 low).

Differential expression was further examined across cancer types with at least five adjacent normal samples. *CXCL1* was significantly upregulated in cholangiocarcinoma (CHOL), colon adenocarcinoma (COAD), esophageal carcinoma (ESCA), head and neck squamous cell carcinoma (HNSC), kidney renal papillary cell carcinoma (KIRP), rectum adenocarcinoma (READ), stomach adenocarcinoma (STAD), thyroid carcinoma (THCA), and uterine corpus endometrial carcinoma (UCEC) (P.adj < 0.05) (Figure 2c), but downregulated in breast invasive carcinoma (BRCA), kidney chromophobe (KICH), liver hepatocellular carcinoma (LIHC), and prostate adenocarcinoma (PRAD) (P.adj < 0.05). *CXCL8* showed a similar upregulation pattern in CHOL, COAD, ESCA, HNSC, KIRP, READ, STAD, THCA, and UCEC (P.adj < 0.05), and was downregulated only in KICH (P.adj < 0.05) (Figure 2d). *CXCL10* (Figure 2e) was significantly upregulated in bladder urothelial carcinoma (BLCA), BRCA, COAD, ESCA, glioblastoma multiforme (GBM), HNSC, kidney renal clear cell carcinoma (KIRC), LIHC, lung adenocarcinoma (LUAD), lung squamous cell carcinoma (LUSC), PRAD, READ, STAD, and UCEC (P.adj < 0.05), with no significant difference between tumor and adjacent normal tissues in CHOL, KICH, KIRP, and THCA.

3.3. Clinical Correlation Analysis

Survival analysis of *CXCL1/8/10* was performed across 33 tumor types to investigate their tumor-promoting or tumor-suppressive roles. *CXCL1/8/10* expression levels were closely associated with patient prognosis, with the low-expression group generally showing higher survival rates (Figure 3). Specifically, low *CXCL1* expression correlated with better overall prognosis in KIRC, LGG, CESC, GBM, and LIHC, while high *CXCL1* expression was associated with better prognosis in COAD and MESO. Low *CXCL8* expression predicted better outcomes in CESC, KIRC, LIHC, and UVM, with high *CXCL8* expression beneficial only in COAD. For *CXCL10,* low expression was favorable in OV, PAAD, SKCM, and UVM, but conversely predicted poorer prognosis in HNSC, KIRP, LAML, LGG, THCA, and THYM. These findings indicate that the prognostic implications of *CXCL1/8/10* differ substantially across tumor types, and that the same gene can have opposing prognostic directions in different cancers.

Cox regression was further applied to analyze the relationship between *CXCL1/8/10* expression and overall survival, using HR > 1 as the threshold for unfavorable prognosis. Univariate Cox regression showed that *CXCL1* expression was associated with favorable prognosis in BRCA, COAD, and MESO (HR < 1), while acting as a risk factor in ACC, CESC, GBM, KIRC, LIHC, THCA, and UVM (HR > 1). For *CXCL10*, it acts as a protective factor (HR < 1) in KIRP, OV and SKCM, but becomes a risk factor (HR > 1) in LAML, LGG, PAAD, THYM and UVM. In summary, *CXCL1, CXCL8* and *CXCL10* are expected to become potential

indicators for predicting tumor progression in clinical settings (Figure 4a).

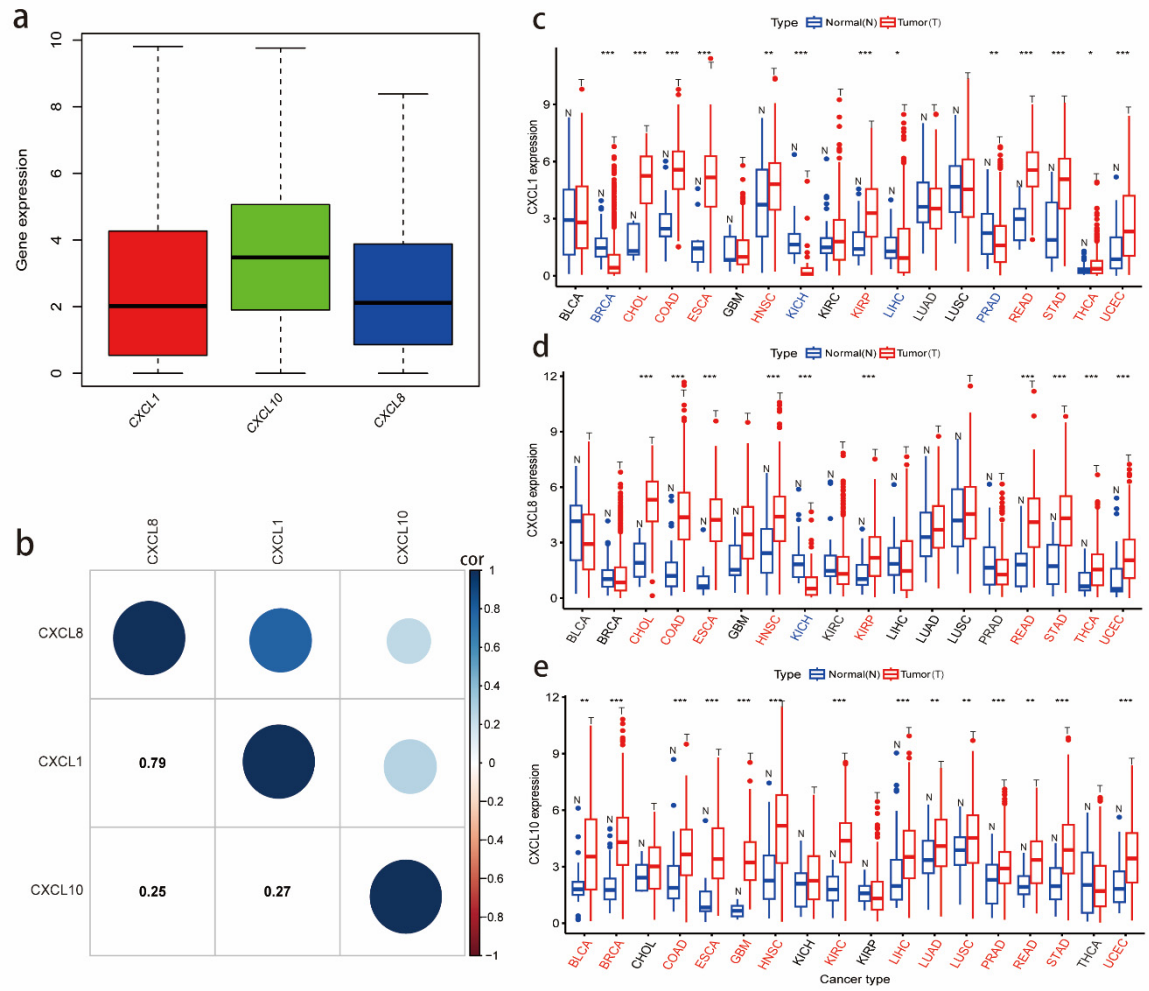

Figure 2. Expression of CXCL1/8/10 in pan-cancer tissues

Box plots showing mRNA abundance distribution of *CXCL1/8/10* across 33 cancer types. (b) Spearman correlations among *CXCL1/8/10* across 33 tumor types. (c) *CXCL1*, (d) *CXCL8*, (e) *CXCL10* differential expression between tumor and adjacent normal tissues. T, tumor tissue; N, adjacent normal tissue. *P < 0.05, **P < 0.01, ***P < 0.001.

3.4. Relationship between *CXCL1/8/10* and TME/Stemness Scores

To explore the relationship between *CXCL1/8/10* and the tumor microenvironment, this study analyzed the expression levels of these genes in 33 types of tumors and their correlations with stromal scores, immune scores, and tumor purity. The results showed that in most tumors, the expression of *CXCL1/8/10* was positively correlated with stromal scores and immune scores (Figure 4b, c), suggesting that their high expression might be related to the enrichment of immune cells and stromal components in tumor tissues. At the same time, the expression of *CXCL1/8/10* was negatively correlated with the purity of various tumors (Figure 4d), indicating that the expression of these genes might be partially derived from stromal cells and immune cells in tumor tissues.

This study, based on RNAss and DNAss, explored the relationship between *CXCL1/8/10* and the stem cell scores of 33 cancer types. Both RNAss and DNAss are indicators for assessing tumor stemness, with higher values indicating stronger stem cell characteristics and lower differentiation levels of tumor cells. The results showed that in most tumors, the expression of *CXCL1/8/10* was negatively correlated with RNAss (Figure 4e), meaning that when gene expression increased, RNAss decreased, suggesting that high expression of *CXCL1/8/10* may be accompanied by weakened tumor stem cell characteristics and increased differentiation level. However, in SARC and HNSC, there was no significant correlation between the expression of *CXCL1/8* and RNAss.

The association between *CXCL1/8/10* and DNAss varies depending on the type of tumor (Figure 4f). In GBM, BLCA, and HNSC, *CXCL1/8/10* is negatively correlated with DNAss, meaning that when the gene expression level increases, DNAss decreases, suggesting a weakened stem cell characteristic and an increased degree of differentiation. In ACC, OV, and CHOL and other tumors, *CXCL1/8/10* is positively correlated with DNAss, meaning that when the gene expression level increases, DNAss increases, suggesting an enhanced stem cell characteristic and a decreased degree of differentiation.

3.5. Relationship between *CXCL1/8/10* Expression and Immune Subtypes/TMB/MSI

The Kruskal-Wallis test was used to analyze the association between *CXCL1/8/10* expression and tumor immune subtypes. *CXCL1/8/10* showed significant associations with six immune subtypes across multiple cancers (P < 0.001) (Figure

5a), with similar expression profiles across the subtypes: highest expression in C2 (IFN-gamma dominant), followed by C1 (wound healing) and C6 (TGF-beta dominant), and lowest in C4 (lymphocyte depleted) and C5 (immunologically quiet). These patterns suggest that *CXCL1/8/10* may participate in regulating the tumor immune microenvironment.

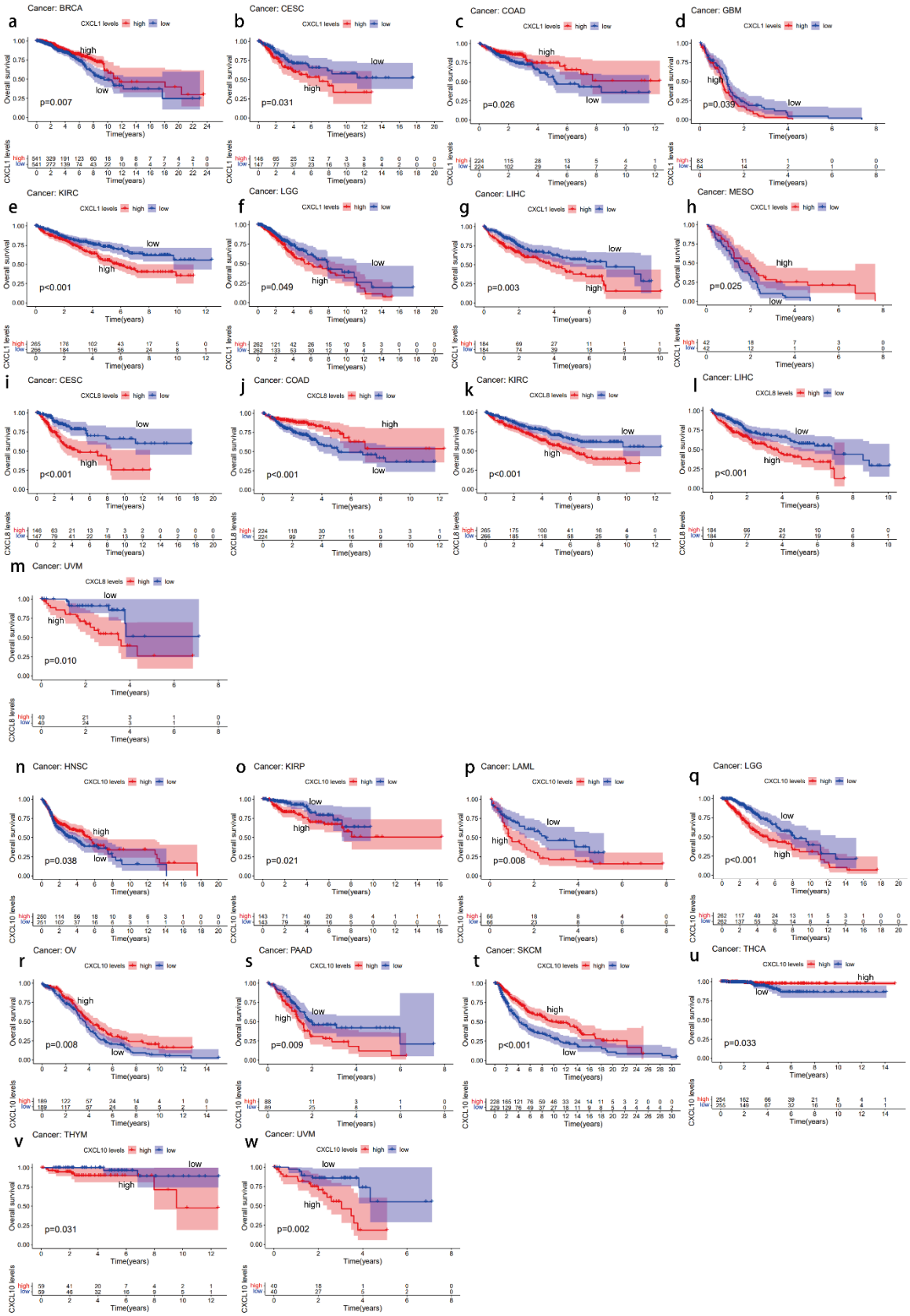

Figure 3. Kaplan-Meier survival curve comparisons of high- and low-expression groups for CXCL1/8/10 in pan-cancer

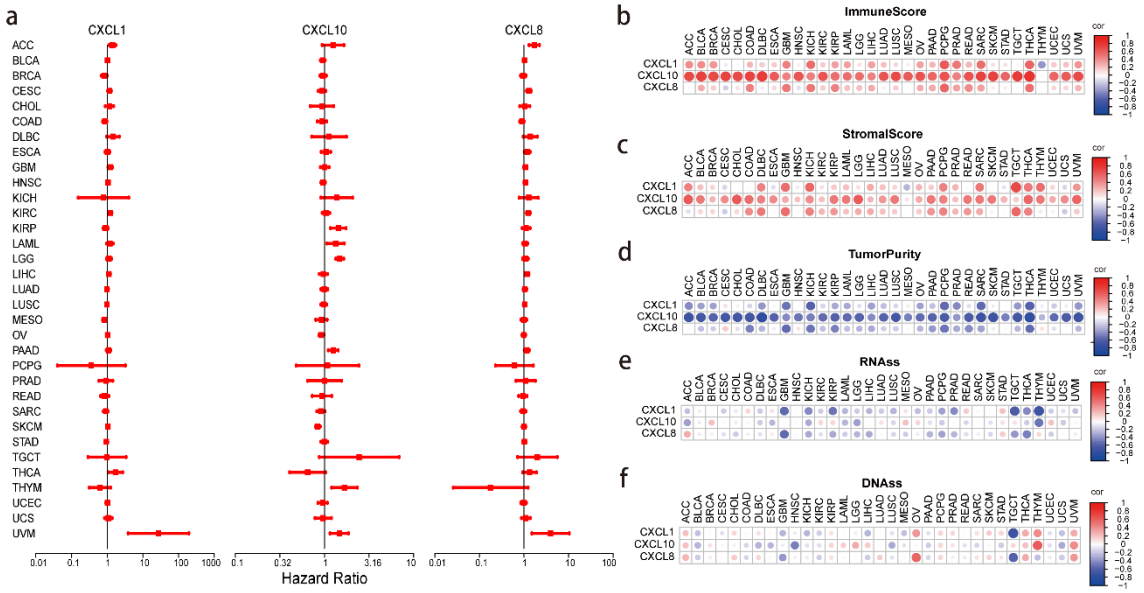

Figure 4. Correlations of CXCL1/8/10 expression with Cox hazard ratios, immune/stromal scores, tumor purity, and RNA/DNA stemness scores across tumors

(a) Cox regression hazard ratios (HR) for *CXCL1/8/10* across cancer types; HR < 1 indicates low risk, HR > 1 high risk. (b-d) Spearman correlations of *CXCL1/8/10* expression with stromal scores, immune scores, and tumor purity. (e-f) Spearman correlations of *CXCL1/8/10* with RNAss and DNAss. RNAss, RNA stemness score; DNAss, DNA stemness score.

After controlling for tumor purity, the association between *CXCL10* expression and TMB proved cancer-type-dependent: significant positive correlations were observed in STAD, BRCA, COAD, SKCM, and THYM, suggesting that aberrant *CXCL10* expression may relate to elevated mutation burden in these tumors. Significant negative correlations with TMB were found in TGCT, HNSC, KIRP, and THCA (Figure 5b).

In the MSI analysis, after adjusting for tumor purity, *CXCL10* expression was significantly and negatively correlated with MSI in TGCT, MESO, and LUSC, while showing positive correlations in UCEC and COAD (Figure 5c), suggesting that *CXCL10* may participate in DNA mismatch repair or cell cycle regulation in these tumors.

4. Discussion

CXC chemokines are small secreted cytokines that regulate immune cell migration and activation, playing important roles in inflammatory responses and tumor immunity [1]. In this study, the gene structure and motifs of representative members of the *CXCL* family were analyzed first, revealing obvious structural differences among different subgroups, which might be related to functional differentiation. Subsequently, the expression characteristics, prognostic value, and association with the tumor microenvironment of *CXCL1/8/10* in 33 types of cancer were systematically analyzed.

CXCL1/8/10 exhibited marked expression heterogeneity across tumor types, and the prognostic direction of the same gene was inconsistent across different cancers. This phenomenon may be related to differences in the immune microenvironment and driver gene mutation backgrounds among tumor types. Taking *CXCL10* as an example, in immune "hot" tumors (such as SKCM), high expression of *CXCL10* may reflect active T-cell infiltration and anti-tumor immunity, thus being associated with a better prognosis; while in immune "cold" tumors or those with stronger immune suppression, the continuous expression of *CXCL10* may participate in immune exhaustion or the chronic inflammatory process promoting tumor growth, thereby being associated with a poor prognosis. Specifically, *CXCL10* not only promotes tamoxifen resistance through estrogen-dependent and -independent pathways in BRCA, but also activates Akt phosphorylation in BRCA cells (such as MCF7), participating in the Akt signaling pathway and promoting tumor progression [11]. In SKCM, the expression of *CXCL10* is closely related to the immune subtype (high expression in C2 subtype, low expression in C4 subtype), and can be used as a potential marker for differentiating immune subtypes; it is highly expressed in the primary and metastatic foci of SKCM and is negatively correlated with patient survival rate [12]. The expression level of CXCR3 on peripheral T cells can serve as a predictive marker for anti-PD-1 therapy response, and intratumoral supplementation of *CXCL10* can increase the proportion of CXCR3+ T cells in the TME, synergistically enhancing the antitumor efficacy of anti-PD-1 antibodies [13].

In STAD, *CXC* chemokines and their receptors play a crucial role in the pathogenesis and development of the disease [14]. The concentrations of *CXCL1/8/10* in the tumor-draining blood and peripheral blood of recurrent patients are significantly increased, and reducing their expression can inhibit the cell migration ability. In EB virus-related STAD, the expression changes of *CXC* chemokines are closely related to the clinical stage, viral infection, and prognosis [15-17]. STAD cells release TNF-alpha to stimulate macrophage secretion of *CXCL1,* which activates a CXCR2-STAT3 positive feedback loop that accelerates tumor cell migration and dissemination, suggesting that targeting *CXCL1* may represent an effective strategy for inhibiting STAD progression and metastasis.

In cancer transcriptome analysis, studies on immune-related genes must take into account the influence of tumor sample purity, as immune cells are the main component of non-cancer cells [18,19]. This study found that in most

cancers, the expression levels of *CXCL1/8/10* were negatively correlated with tumor purity, suggesting that the expression of these genes may be partially derived from immune cells and stromal cells in tumor tissues. In TMB/MSI analysis, this study used Spearman partial correlation analysis to control for tumor purity, and the results showed that the correlation between *CXCL10* and TMB/MSI remained significant after correction in some cancer types, while the correlation weakened in other cancer types, indicating that some previous associations may be confounded by tumor purity [20,21]. This result suggests that when analyzing the relationship between the expression of immune-related genes and mutation burden, it is necessary to correct for tumor purity to avoid false correlations.

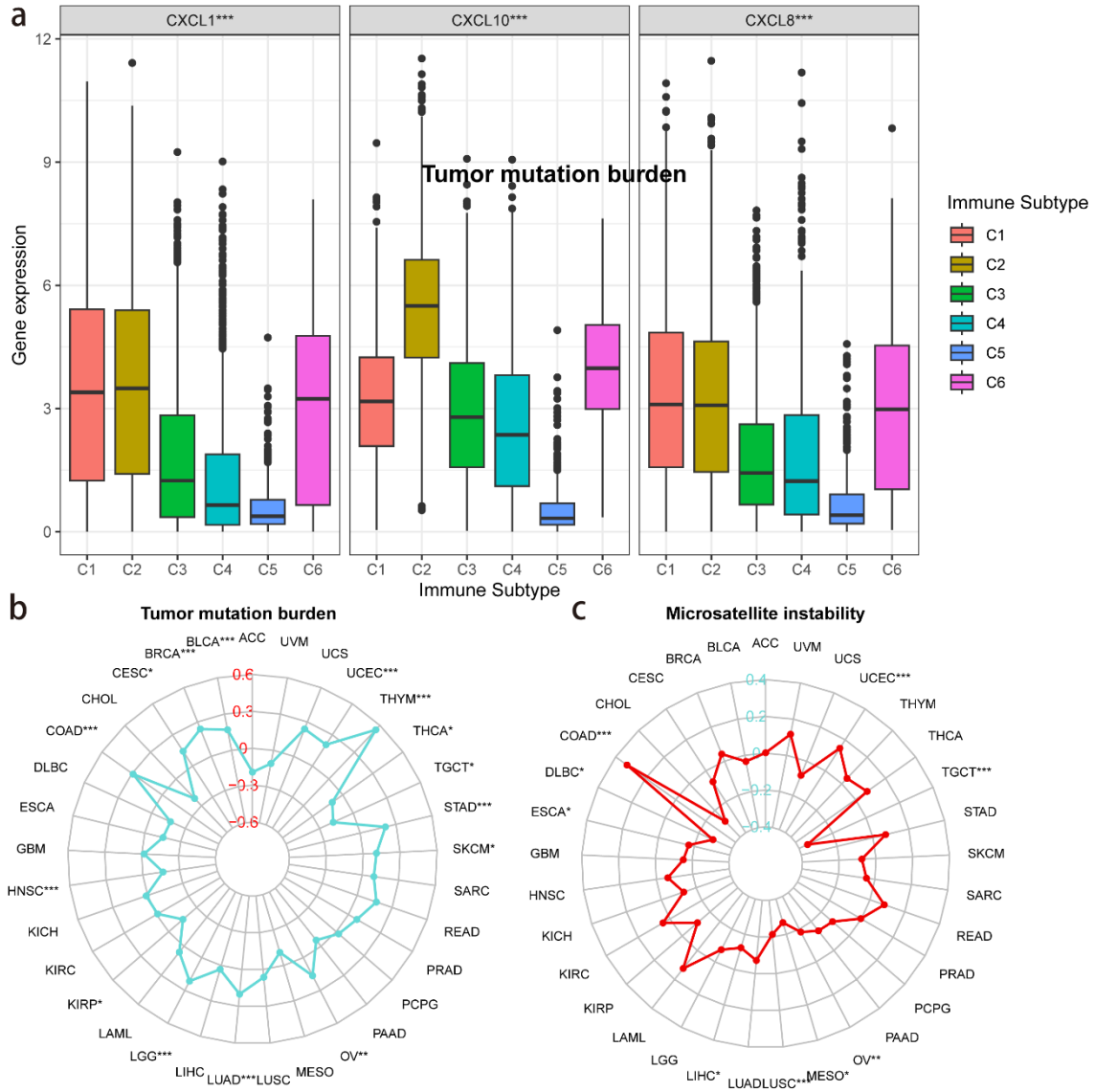

Figure 5. Expression levels of *CXCL1/8/10* across immune subtypes and correlation analysis of CXCL10 with TMB and MSI in pan-cancer

(a) Expression of *CXCL1/8/10* across immune subtypes in pan-cancer. X-axis: immune subtype; Y-axis: gene expression (log2(FPKM+1)). C1, wound healing; C2, IFN-gamma dominant; C3, inflammatory; C4, lymphocyte depleted; C5, immunologically quiet; C6, TGF-beta dominant. *P < 0.05, **P < 0.01, ***P < 0.001. (b) TMB and (c) MSI Spearman partial correlation analysis with *CXCL10* expression (controlled for tumor purity). *P < 0.05, **P < 0.01, ***P < 0.001.

This study has the following limitations. First, this study is based on retrospective data from the TCGA and UCSC Xena public databases, which cannot infer causal relationships, and the TCGA samples are mainly from European and American populations, with racial and regional biases, and the applicability of the results in other populations needs to be verified. Second, the exploration of the specific functional mechanisms of *CXCL1/8/10* is mainly based on correlation analysis, and lacks experimental verification. Finally, although multiple-factor Cox regression was introduced to correct some clinical confounding factors, more clinical samples and external independent datasets are still needed to verify the stability of these biomarkers in different populations.

References

[1] Zhou, C., Gao, Y., Ding, P., & et al. (2023). The role of CXCL family members in different diseases. Cell Death Discovery, 9(1), 212. https://doi.org/10.1038/s41420-023-01476-5.

[2] Hughes, C. E., & Nibbs, R. J. B. (2018). A guide to chemokines and their receptors. The FEBS Journal, 285(16), 2944-2971. https://doi.org/10.1111/febs.14466.

[3] Cabrero-de las Heras, S., & et al. (2018). CXC chemokines as biomarkers in colorectal cancer. World Journal of

Gastroenterology, 24(42), 4738-4749. https://doi.org/10. 3748/wjg. v24. i42.4738.

[4] Zdanowska, N., & et al. (2021). The role of chemokines in psoriasis- an overview. Medicina (Kaunas), 57(8). https://doi. org/ 10. 3390/medicina57080820.

[5] Sun, Y., & et al. (2021). Genome-wide identification of the JAZ gene family in tomato. International Journal of Molecular Sciences, 22(18). https://doi.org/10.3390/ijms22189744.

[6] Han, Y., & Luthe, D. (2021). Identification and evolution analysis of the JAZ gene family in maize. BMC Genomics, 22(1), 256. https://doi.org/10.1186/s12864-021-07572-4.

[7] Waterhouse, A., & et al. (2018). SWISS-MODEL: homology modelling of protein structures and complexes. Nucleic Acids Research, 46(W1), W296-W303. https://doi.org/ 10.1093/ nar/ gky427.

[8] Chen, C., & et al. (2020). TBtools: an integrative toolkit developed for interactive analyses of big biological data. Molecular Plant, 13(8), 1194-1202. https://doi.org/10.1016/ j.molp. 2020.06.009.

[9] Goldman, M. J., & et al. (2020). Visualizing and interpreting cancer genomics data via the Xena platform. Nature Biotechnology, 38(6), 675-678. https://doi.org/10. 1038/ s41 587-020-0546-8.

[10] Malta, T. M., & et al. (2018). Machine learning identifies stemness features associated with oncogenic dedifferentiation. Cell, 173(2), 338-354. https://doi.org/10. 1016/j.cell. 2018. 03. 034.

[11] Wu, X., & et al. (2020). CXCL10 mediates breast cancer tamoxifen resistance and promotes estrogen-dependent and independent proliferation. Molecular and Cellular Endocrinology, 512, 110866. https://doi. org/10. 1016/j. mce. 2020. 110866.

[12] Zhou, X., & et al. (2021). CXC chemokines as therapeutic targets and prognostic biomarkers in skin cutaneous melanoma microenvironment. Frontiers in Oncology, 11, 619003. https:// doi. org/10.3389/fonc.2021.619003.

[13] Gorbachev, A. V., & et al. (2007). CXC chemokine ligand 9/monokine induced by IFN-gamma production by tumor cells is critical for T cell-mediated suppression of cutaneous tumors. Journal of Immunology, 178(4), 2278-2286. https://doi.org/10. 4049/ jimmunol.178.4.2278.

[14] Lee, H. J., & et al. (2014). CXC chemokines and chemokine receptors in gastric cancer: from basic findings towards therapeutic targeting. World Journal of Gastroenterology, 20(7), 1681-1693. https://doi.org/10.3748/wjg.v20.i7.1681.

[15] Miyazaki, H., & et al. (2013). Chemokines, chemokine receptors and the gastrointestinal system. World Journal of Gastroenterology, 19(19), 2847-2863. https://doi.org/10. 3748/wjg. v19.i19.2847.

[16] Kitadai, Y., & et al. (1998). Expression of interleukin-8 correlates with vascularity in human gastric carcinomas. The American Journal of Pathology, 152(1), 93-100.

[17] Torti, D., & et al. (2012). A preclinical algorithm of soluble surrogate biomarkers that correlate with therapeutic inhibition of the MET oncogene in gastric tumors. International Journal of Cancer, 130(6), 1357-1366. https://doi.org/10. 1002/ijc. 26162.

[18] Rhee, J. K., & et al. (2018). Impact of tumor purity on immune gene expression and clustering analyses across multiple cancer types. Cancer Immunology Research, 6(1), 87-97. https://doi. org/ 10.1158/2326-6066.CIR-17-0207.

[19] Aran, D., & et al. (2015). Systematic pan-cancer analysis of tumour purity. Nature Communications, 6, 8971. https://doi. org/ 10.1038/ncomms9971.

[20] Li, B., & et al. (2016). Comprehensive analyses of tumor immunity: implications for cancer immunotherapy. Genome Biology, 17(1), 174. https://doi.org/10. 1186/ s130 59-0 16-1060-7.

[21] Rooney, M. S., & et al. (2015). Molecular and genetic properties of tumors associated with local immune cytolytic activity. Cell, 160(1-2), 48-61. https://doi.org/ 10.1016/j. cell. 2014.12.033.